Journal of Hazardous Materials 511 (2026) 142011

Contents lists available at ScienceDirect

Journal of Hazardous Materials

journal homepage: www.elsevier.com/locate/jhazmat

Indoor atmospheric nanoparticle emissions, inhalation exposures, and indoor-to-outdoor transport during residential activities with electric and combustion appliances

Satya S. Patra [a,b], Chunxu Huang [b], Brian H. Magnuson [b], Brandon E. Boor [b,*], Nusrat Jung [b,*]

[a] Department of Civil, Construction, and Environmental Engineering, University of Alabama, Tuscaloosa, AL 35487, United States
[b] Lyles School of Civil and Construction Engineering, Purdue University, West Lafayette, IN 47907, United States

HIGHLIGHTS

- Electric induction and gas stove cooking both generate ~10^7 nanoparticles cm^{-3}.
- Sub-3 nm nanocluster aerosol is abundant during high-temperature oil-based cooking.
- Daily inhalation dose reaches ~10^{12} nanoparticles under electric and combustion use.
- Indoor-to-outdoor nanoparticle fluxes rival or exceed urban traffic emissions.
- Building electrification alone is unlikely to reduce indoor nanoparticle pollution.

GRAPHICAL ABSTRACT

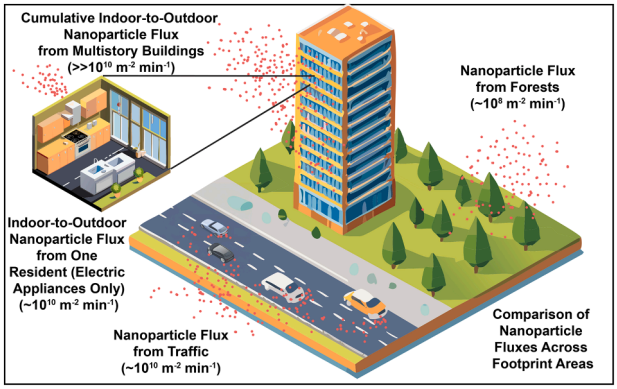

ARTICLE INFO

Keywords:
Indoor air quality
Nanocluster aerosol
Nanoparticle emissions
Inhalation exposure
Indoor-to-outdoor transport
Urban air pollution
Residential electrification

ABSTRACT

Indoor-originated nanoparticles are an emerging class of hazardous airborne contaminants with the capacity to penetrate deep into the respiratory system and translocate to sensitive organs. Use of electric appliances is widely promoted to improve indoor and outdoor air quality, yet their implications for nanoparticle emissions during residential cooking, particularly under oil-based, high-temperature conditions, remain poorly understood. Using a controlled residential test house, we conducted the first size-resolved comparison of nanoparticles down to 1 nm emitted during full-day household activities performed exclusively with combustion- or electric-based appliances. High-temperature, oil-based electric induction cooking generated peak nanoparticle concentrations on the order of 10^7 nanoparticles cm^{-3}, comparable to high-temperature, oil-based gas stove cooking. Both produced abundant sub-3 nm nanocluster aerosol (NCA) that accounted for > 80% of total nanoparticle counts during active emission periods. Across full-day activity cycles, electric and combustion appliances yielded similar cumulative nanoparticle emissions and inhalation exposures, with daily respiratory tract deposited doses reaching approximately 10^{12} deposited nanoparticles under both appliance scenarios. Furthermore, modeled

* Corresponding authors.
E-mail addresses: bboor@purdue.edu (B.E. Boor), nusratj@purdue.edu (N. Jung).

https://doi.org/10.1016/j.jhazmat.2026.142011
Received 27 November 2025; Received in revised form 28 March 2026; Accepted 6 April 2026
Available online 9 April 2026

indoor-to-outdoor nanoparticle fluxes were substantial for both appliance types (10^{12}–10^{13} nanoparticles min^{-1}), and building-footprint-normalized fluxes from electric-appliance use (10^{10}–10^{11} nanoparticles m^{-2} min^{-1}) exceeded reported urban traffic nanoparticle fluxes. These findings demonstrate that non-combustion, thermally driven processes can generate intense bursts of indoor atmospheric nanoparticles and NCA, challenging the assumption that residential electrification universally reduces nanoparticle pollution. Effective mitigation strategies must therefore address primary and secondary nanoparticle sources in residential environments and the size-dependent exposure and indoor-to-outdoor transport processes revealed here.

1. Introduction

Indoor air pollutant emissions do not stay indoors: they are vented outdoors, where they add to urban air pollution burdens. A recent study reported that residential electrification in California, U.S. reduced air pollutant emissions and ambient fine particulate matter concentrations [1]; however, those reductions were inferred mainly from decreases in nitrogen oxides, even though particles can also arise from heated organics [2] that do not produce nitrogen oxides. Thus, the extent to which electrification delivers the expected reductions in ambient particle concentrations remains uncertain. Moreover, while interest in electric appliances is often driven by the belief that they improve air quality, their effectiveness in reducing indoor atmospheric nanoparticle emissions has not been systematically assessed under typical residential conditions. Most Americans (60%) prefer homes in which major appliances are powered by electricity, according to a recent nationally representative survey, underscoring growing interest in residential electrification [3]. Quantifying the impact of electrification on ambient nanoparticle pollution in urban environments therefore requires direct, field-based measurements comparing combustion and electric appliances.

Combustion appliances indeed produce substantial concentrations of indoor-originated nanoparticles, including nanocluster aerosol (NCA; nanoparticles smaller than 3 nm) [4,5]. In response, electric induction cooktops have gained attention as cleaner alternatives, presumed to eliminate combustion-related pollutants. However, the smallest nanoparticle size characterized during isolated induction cooking is approximately 5.6 nm [6], leaving potentially significant emissions of smaller NCA unexamined. This gap in characterization may lead to a substantial underestimation of total indoor-originated nanoparticles released from electric induction cooking, especially given recent findings suggesting that most indoor-originated nanoparticles emitted during active emission periods fall within the sub-3 nm NCA size range [4,7,8]. This previously uncharacterized size range presents unique health concerns due to their high deposition rates within the human respiratory tract, their ability to penetrate biological membranes, and potential systemic translocation to vital organs [4,9,10].

Beyond residential cooking appliances, indoor atmospheric nanoparticle emissions are influenced by numerous other everyday activities involving fragranced chemical products, such as cleaning agents, skin and hair care products, scented candles, and air fresheners [2,7,8,11–14]. Recent research underscores that scented volatile chemical products (sVCPs), through reactions with indoor atmospheric oxidants like ozone, can generate substantial amounts of indoor atmospheric nanoparticles [7]. While such secondary nanoparticle formation has been acknowledged, systematic evaluations of how substituting combustion-based sVCPs (for example, scented candles) with electric alternatives (such as wax warmers) affects nanoparticle emissions are still lacking. Additionally, most previous studies have examined indoor-originated nanoparticle emissions from these products in isolation, neglecting their potential interactions when multiple emission sources coexist in realistic home scenarios.

In this study, we provide the first comprehensive and systematic assessment of indoor-originated nanoparticle emissions, inhalation exposures, and indoor-to-outdoor nanoparticle fluxes from everyday household activities, comparing combustion-based sources against electric-based alternatives within a fully controlled residential environment. By employing a two-stage particle size magnifier–scanning mobility particle sizer (PSMPS) [15], we measured indoor-originated nanoparticles across a broad size range, detecting indoor atmospheric nanoparticles as small as 1 nm. We conducted typical daily activities such as high-temperature, oil-based cooking, cleaning, and using scented consumer products, comparing days that exclusively used either combustion- or electric-based appliances. This approach allowed us to capture the complex, dynamic nature of indoor-originated nanoparticle emissions, inhalation exposures, and indoor-to-outdoor nanoparticle transport, and to assess whether electric alternatives provide a meaningful reduction in nanoparticle pollution under the conditions examined in the study.

2. Materials and methods

2.1. Experimental design

We assessed indoor-originated nanoparticle emissions from both combustion- and electric-based appliances within the Purdue zero Energy Design Guidance for Engineers (zEDGE) test house (interior volume = 60.35 m^3) [2,4,7,8,11–14]. A ductless single-zone heating and cooling system (Model FTX12NMVJU, Daikin North America LLC, Houston, TX, U.S.) and a portable air conditioning unit with an exhaust duct (Model QPCA08JAMWG1, Haier, Louisville, KY, U.S.) maintained climate control of the test house (nominal indoor air temperature = 20°C (68 °F)). The test house also features a variable-speed powered ventilator equipped with dual MERV 13 filters, allowing for the intake of filtered outdoor air. Ventilation settings on both the powered ventilator and the portable air conditioning unit were adjusted to achieve targeted outdoor air exchange rates, which were monitored daily using a carbon dioxide (CO_2) tracer gas injection and decay method. To ensure uniform air distribution, four mixing fans were deployed throughout the interior volume of the test house. Previous tests confirmed that indoor atmospheric nanoparticle concentrations were well mixed under these conditions [4].

We conducted activities in the test house under two categories: isolated stove use and full-day realistic household activities. The isolated stove use activities included boiling water and cooking grilled cheese sandwiches. The procedure for boiling water and cooking grilled cheese sandwiches is detailed in Patra et al. [4]. Each activity was conducted once using a propane gas stove and once using an electric induction stove, with two occupants in the test house. The test house features a kitchen area where the induction stove is installed. For activities involving the propane gas stove, the same kitchen area was used by placing the gas stove on top of the induction stove, with the induction stove covered. The electric induction stove settings were selected to raise the water temperature to the same level in the same amount of time as the gas stove. Each isolated stove use activity was repeated in triplicate. The nominal outdoor air ventilation rate for all twelve of these isolated stove use activities was 0.4 air changes h^{-1}.

In addition to the twelve isolated stove use activities, we conducted three additional (in triplicate) isolated boiling water activities using the gas stove, with the kitchen exhaust hood turned on. The kitchen exhaust hood in the test house (Model UXW7324BSS1, Whirlpool Corporation, Benton Harbor, MI, U.S.) is a variable-speed unit with three settings,

venting indoor air to the outdoors. The volumetric airflow rates for all three settings are shown in Figure S1. For this activity, the kitchen exhaust hood was operated at the medium flow setting. All fifteen isolated stove use activities included a 10-minute background period with occupants present and no activities performed, a 20-minute stove-active period, and a 120-minute nanoparticle decay period.

The full-day realistic household activities included typical tasks commonly performed in homes, such as cooking, cleaning, and using personal care products. A key feature of our approach was that we repeated the same set of activities on two separate days, once using only combustion-based appliances and once using only electric-based appliances. This allowed for a direct comparison of indoor-originated nanoparticle emissions between the two energy sources. Occupancy in the test house ranged from zero to a maximum of four people, reflecting typical household patterns. We carried out these activities in a manner consistent with how they would naturally occur in a real home. The nominal outdoor air ventilation rate was 6.5 air changes h^{-1} on both days. Table S1 summarizes the activities performed on the combustion-based appliance day, and Table S2 summarizes those from the electric-based appliance day.

2.2. Online indoor atmospheric nanoparticle measurements

We used two state-of-the-art indoor atmospheric nanoparticle detection technologies: a standard scanning mobility particle sizer (SMPS) and a newly commercialized two-stage particle size magnifier–scanning mobility particle sizer (PSMPS). These instruments facilitated direct measurements of indoor-originated nanoparticles in real-time during all isolated stove use and full-day realistic household activities in the test house.

The newly commercialized PSMPS is capable of electrical-mobility-based atmospheric nanoparticle measurements as small as 1 nm [15]. It combines several specialized components: a soft X-ray neutralizer (Model 5524-X, GRIMM Aerosol Technik Ainring GmbH & Co. KG, Ainring, Germany), a modified short Vienna-type differential mobility analyzer (S-DMA; GRIMM Aerosol Technik Ainring GmbH & Co. KG, Ainring, Germany), a diethylene glycol-based particle size magnifier (Model A10, Airmodus Ltd., Helsinki, Finland), and a butanol-based condensation particle counter (Model 5417, GRIMM Aerosol Technik Ainring GmbH & Co. KG, Ainring, Germany). The instrument captures a new nanoparticle number size distribution every 120 s. Patra et al. [4] provide a detailed overview of its configuration and operation.

The standard SMPS comprised a Kr-85 bi-polar charger (370 MBq, Model 3077 A, TSI Inc., Shoreview, MN, U.S.), a long differential mobility analyzer (Model 3081, TSI Inc., Shoreview, MN, U.S.), and a water-based condensation particle counter (Model 3788, TSI Inc., Shoreview, MN, U.S.) [16,17]. It enabled similar electrical-mobility-based measurements of indoor atmospheric nanoparticles and recorded a new nanoparticle number size distribution every 120 s. In this study, the lower and upper detection limits for indoor-originated nanoparticles were 13.1 nm and 572.5 nm for the standard SMPS, and 1.26 nm and 51.4 nm for the PSMPS. Figure S2 shows the layout of the indoor-originated nanoparticle measuring instruments in the test house.

2.3. Indoor atmospheric nanoparticle data analysis

We merged indoor-originated nanoparticle number size distributions from both the SMPS and PSMPS using a weighted average in the overlapping size range (13.1–51.4 nm) to obtain continuous, wide-range indoor-originated nanoparticle size distributions from 1.26 to 572.5 nm. The standard SMPS and PSMPS have been reported to agree well with each other in the overlapping size range [4]. For example, in our measurements of a representative gas stove combustion event, the correlation coefficients between the two instruments were 0.94, 0.99, and 0.94 during the background, active combustion, and post-combustion periods, respectively, confirming consistent agreement across all phases.

PSMPS measurements in the sub-3 nm NCA size range are influenced by instrument-generated charger ions [4,18,19]. Previous studies have developed a data-driven correction method that uses a threshold value derived from background and decay measurements [4,7]. For isolated stove use activities, we applied a similar charger ion correction method using the 99th percentile of sub-3 nm NCA number size distributions measured during the background period and at the end of the decay period.

In contrast, full-day realistic household activities did not feature distinct background and decay periods. Therefore, we used time periods prior to specific emission events, when no activities were occurring, to calculate the 99th percentile threshold for charger ion correction of the subsequent activity (Figure S3). Using a high 99th percentile threshold increases confidence in the corrected sub-3 nm NCA number size distribution [20]. Details of the charger ion correction method are available elsewhere [4,7]. All indoor-originated nanoparticle number size distributions presented and used in the subsequent analysis underwent sub-3 nm charger ion correction. We size-integrated the charger ion-corrected indoor-originated nanoparticle number size distributions across specific size fractions to obtain nanoparticle counts within defined ranges. Throughout the analysis, three size-integration intervals were used: nanocluster aerosol (NCA; 1.26–3 nm), 3–100 nm, and 100–500 nm.

Indoor-to-outdoor nanoparticle fluxes [$\Phi_{I\to O}$; nanoparticles min^{-1}] for the full-day activities were estimated using Eq. 1 [21]:

$$\Phi_{I\to O} = \int_{1.26\ nm}^{572.5\ nm} \left(\frac{dN}{dlogD_{em}} \bullet \frac{k_{vent}}{60} \bullet V \bullet \eta_{D_{em}} \right) \bullet dlogD_{em} \quad (1)$$

In Eq. 1, $\frac{dN}{dlogD_{em}}$ $[cm^{-3}]$ is the charger ion-corrected indoor-originated nanoparticle number size distribution, k_{vent} $[h^{-1}]$ is the nominal outdoor air ventilation rate (6.5 air changes h^{-1}), V $[cm^3]$ is the volume of the test house, and $\eta_{D_{em}}$ is the size-dependent indoor-originated nanoparticle transmission efficiency through the kitchen exhaust pathway. $\eta_{D_{em}}$ was modeled based on turbulent diffusive nanoparticle losses in the kitchen exhaust pathway, as described in Eqs. 2–4 [22]:

$$\eta_{D_{em}} = e^{-\xi_{D_{em}} \bullet Sh_{D_{em}}} \quad (2)$$

where,

$$\xi_{D_{em}} = \frac{\pi \bullet D_{D_{em}} \bullet L}{Q} \quad (3)$$

and

$$Sh_{D_{em}} = 0.0118 \bullet \mathrm{Re}_f^{\frac{7}{8}} \bullet Sc_{D_{em}}^{\frac{1}{3}} \quad (4)$$

Re_f is the airflow Reynolds number; $Sc_{D_{em}}$ is the nanoparticle Schmidt number [22]; Sh_{Dem} is the nanoparticle Sherwood number [22]; $D_{D_{em}}$ is the nanoparticle diffusion coefficient, estimated using the Stokes–Einstein–Sutherland relation (with Cunningham slip correction) [23]; Q is the kitchen exhaust volumetric airflow rate, estimated using the volume of the test house and the nominal outdoor air ventilation rate; and L is the kitchen exhaust pathway length; in this analysis, a conservative value corresponding to the maximum recommended by ANSI/ASHRAE Standard 62.1(8 m with 3 elbows) was assumed, yielding an equivalent length of 15 m. We intentionally adopted a conservative transport assumption; therefore, the estimated fluxes reported here can be interpreted as a lower bound of indoor-originated nanoparticle fluxes to the outdoor environment. The resulting conservative, size-dependent transmission efficiency for indoor-originated nanoparticles is shown in Figure S4.

Finally, we quantified indoor-originated nanoparticle inhalation exposure risks by calculating cumulative respiratory tract deposited doses across three distinct regions of the adult respiratory tract: head

airways, tracheobronchial region, and pulmonary region. We followed established methods from the literature [24,25]. Briefly, we calculated size-resolved respiratory tract deposited dose rates by multiplying the measured indoor-originated nanoparticle number size distributions by the inhalation rate and the size-resolved nanoparticle deposition fractions for each respiratory tract region. We obtained deposition fractions for an adult using the age-specific open-source Multiple-Path Particle Dosimetry (MPPD) model (v3.04, Applied Research Associates Inc., Albuquerque, NM, U.S.) [26]. We then integrated the size-resolved respiratory tract deposited dose rates over the 1.26–500 nm size range and over time to determine the cumulative respiratory tract deposited doses.

3. Results and discussion

3.1. Indoor atmospheric nanoparticle emissions during isolated cooking activities: stove type comparisons and kitchen exhaust hood effectiveness

We directly measured indoor-originated nanoparticle emissions down to ~1 nm in a residential test house (the Purdue zEDGE test house) designed to accommodate both propane gas and electric induction stoves. Indoor-originated nanoparticles were characterized using a standard SMPS and a recently developed two-stage PSMPS, which enabled real-time detection and sizing of nanoparticles as small as 1 nm. To evaluate stove-specific emissions, we compared nanoparticles released into air during two selected cooking activities, boiling water and cooking grilled cheese sandwiches, under identical isolated conditions. This study provides the first size-resolved assessment of indoor atmospheric nanoparticle emissions during electric induction cooking with measurements extending down to 1 nm.

High-temperature, oil-based cooking on the electric induction stove significantly elevated indoor atmospheric nanoparticle concentrations, with nanoparticle counts in the 1.26–500 nm size range exceeding 10^7 nanoparticles cm^{-3}, more than 2000 times above the background level (~5×10^3 nanoparticles cm^{-3}) (Fig. 1, bottom row). These emissions primarily resulted from high-temperature butter cooking during the preparation of grilled cheese sandwiches [27]. Notably, nanoparticle release was delayed until the pan reached temperatures sufficient to trigger fat breakdown, likely producing glycerol and free fatty acids [28,29]. These compounds can further decompose into lower-volatility organics that serve as precursors for nanoparticle formation [30–32]. The emitted nanoparticles persisted in indoor air at high concentrations, with nanoparticles as small as 1 nm staying both stable and abundant during the cooking period (Fig. 1, bottom row).

Interestingly, boiling water on the electric induction stove did not generate any detectable indoor atmospheric nanoparticles (Fig. 1, top row), highlighting that high-temperature, fat-based cooking specifically drives nanoparticle formation with electric induction stoves. Therefore, the electric induction stove itself is not a direct source of nanoparticles; rather, oil-based cooking on the induction stove generates indoor

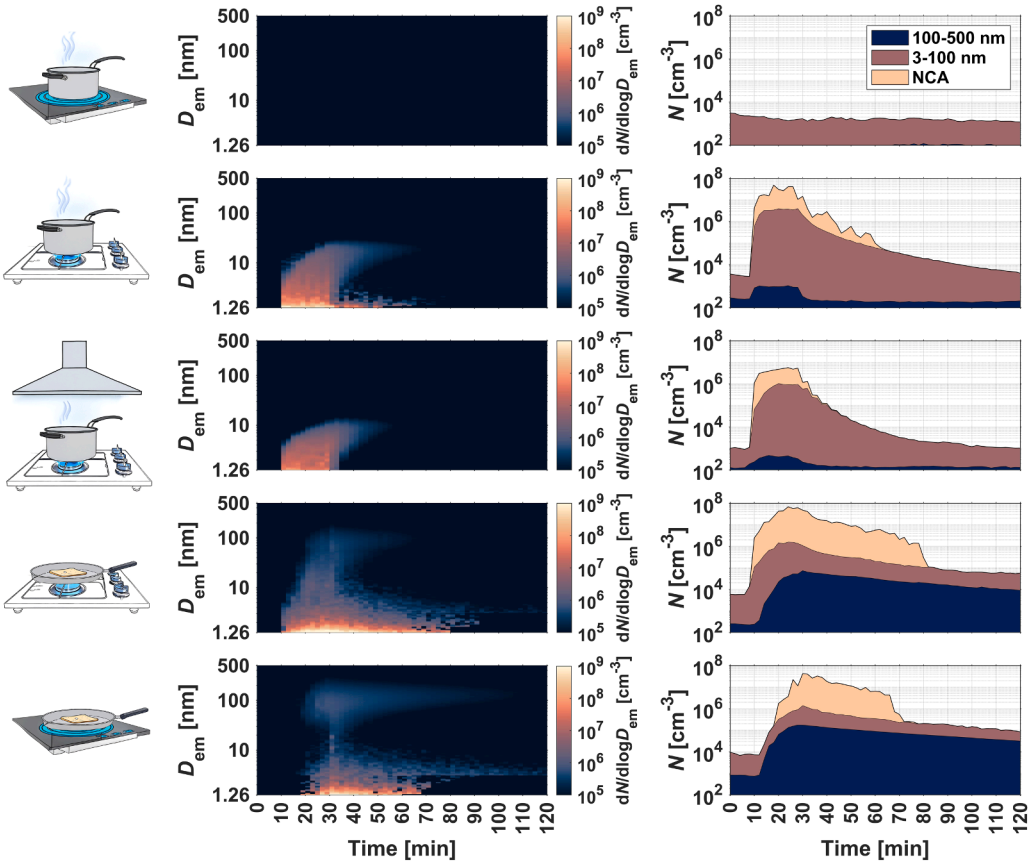

Fig. 1. Time-resolved evaluation of indoor-originated nanoparticle emissions from isolated electric induction and gas stove use. The nanoparticle number size distributions in the left column present representative examples, while the size-integrated nanoparticle number concentrations in the right column show median values across similar activities. These activities include: (top row) boiling water on the electric induction stove; (second row) boiling water on the gas stove; (third row) boiling water on the gas stove with the kitchen exhaust hood operating at the medium setting (~167 ft^3 min^{-1} (283 m^3 h^{-1})); (fourth row) cooking grilled cheese sandwiches on the gas stove; and (bottom row) cooking grilled cheese sandwiches on the electric induction stove. The size-integrated number concentrations are color-coded according to their corresponding size-integration intervals: nanocluster aerosol (NCA; 1.26–3 nm), 3–100 nm, and 100–500 nm. In each activity, the stove was turned on at the 10-minute mark. The nanoparticle number size distributions for all fifteen isolated electric induction and gas stove use activities (triplicates of each of the five categories) are presented in Fig. S5.

atmospheric nanoparticles. Gas stoves, in contrast, are widely recognized nanoparticle sources due to the presence of an open flame, which directly emit indoor atmospheric nanoparticles as small as 1 nm [4,5]. Consistent with previous findings, we observed substantial indoor atmospheric nanoparticle emissions from gas stoves during both boiling water and cooking grilled cheese sandwiches (Fig. 1, second and fourth rows). However, under fat-based, high-temperature cooking conditions, indoor-originated nanoparticle emissions from the electric induction stove reached concentrations comparable to those from the gas stove, suggesting that emissions are also driven by the cooking process rather than the energy source alone (Fig. 2, left column).

Peak nanoparticle concentrations while cooking grilled cheese sandwiches were of similar order of magnitude across stove types ($\sim 9 \times 10^7$ nanoparticles cm^{-3} for the gas stove, $\sim 4 \times 10^7$ nanoparticles cm^{-3} for the electric induction stove). These results challenge the common assumption in policy discussions that replacing gas stoves with electric induction alternatives inherently eliminates nanoparticle emissions. While electric induction stoves remove flame-related nanoparticle emissions (as confirmed by negligible nanoparticles detected during water boiling on the induction stove), they do not necessarily result in lower nanoparticle levels during the high-temperature, oil-based cooking conditions examined in this study. The comparable emissions observed between gas and electric induction cooking under these conditions suggest that nanoparticle formation is also driven by cooking processes, particularly the thermal decomposition of oils, rather than the energy source alone. These findings highlight the importance of considering cooking-related emissions when evaluating indoor nanoparticle exposures in residential environments.

NCA, nanoparticles measuring 1–3 nm in diameter, represent an understudied yet significant class of indoor-originated nanoparticles with unique health implications due to their high respiratory deposition and potential translocation from the lungs to other organs, including the brain [9,10]. Typically, NCA emissions are associated with combustion processes or oxidation of reactive gases such as terpenes [4,7,8]. Here, we identify a prevalent but previously unrecognized NCA source: high-temperature, fat-based cooking, even without combustion. During gas stove use, NCA arise both directly from flames and indirectly from cooking processes, evident from their release during both water boiling and grilled cheese sandwich cooking (Fig. 2, middle column). By contrast, electric induction stoves emit NCA exclusively during high-temperature, fat-based cooking, as no NCA were detected during water boiling (Fig. 2, middle column). Remarkably, sub-3 nm NCA emissions exceeded 10^7 NCA cm^{-3} for both stove types during high-temperature, oil-based cooking, comprising over 80% of total indoor-originated nanoparticle counts (Fig. 2, middle and right columns). These results indicate that NCA originate from two distinct indoor sources: combustion processes and high-temperature, oil-based cooking. The latter is confirmed as an independent source by the absence of NCA during induction water boiling, with intense emissions arising under high-temperature, fat-based cooking conditions regardless of energy source.

Using a kitchen exhaust hood is widely recommended to reduce the persistence of indoor air pollutants during stove operation [33,34]. In our study, kitchen exhaust hood use reduced indoor-originated nanoparticle concentrations, including the sub-3 nm NCA size fraction, by approximately 85% (Fig. 1, third row; Fig. 2, left and middle columns; see Section 2.1 for kitchen exhaust hood details). However, due to the magnitude of nanoparticle emissions, indoor nanoparticle levels still exceeded 10^6 nanoparticles cm^{-3} even after this reduction. Kitchen exhaust hood use, however, primarily transfers the nanoparticle burden from indoor to outdoor air, forming an important outdoor nanoparticle source that exacerbates urban atmospheric nanoparticle concentrations (see Section 3.4). Thus, while kitchen exhaust hoods substantially lower indoor nanoparticle concentrations, exposure can remain elevated due to the magnitude of nanoparticle emission rates, and hood use alone may be insufficient to fully mitigate indoor exposure risks.

Collectively, the findings discussed in this section refine our understanding of nanoparticle emissions from high-temperature, oil-based cooking. While this section focused on isolated cooking events, the next explores how indoor-originated nanoparticle emissions evolve across the full span of a day, considering both combustion and electric alternatives.

3.2. *Combustion vs. electric household appliances: real-world comparison reveals complex indoor-originated nanoparticle pollution trade-offs*

Isolated cooking activities demonstrated comparable nanoparticle emissions between electric induction and gas stoves under high-temperature, oil-based cooking conditions, suggesting that the cooking process itself, rather than energy source alone, drives emissions. However, isolated activities cannot capture the complete picture of daily residential nanoparticle pollution. Therefore, we used the Purdue

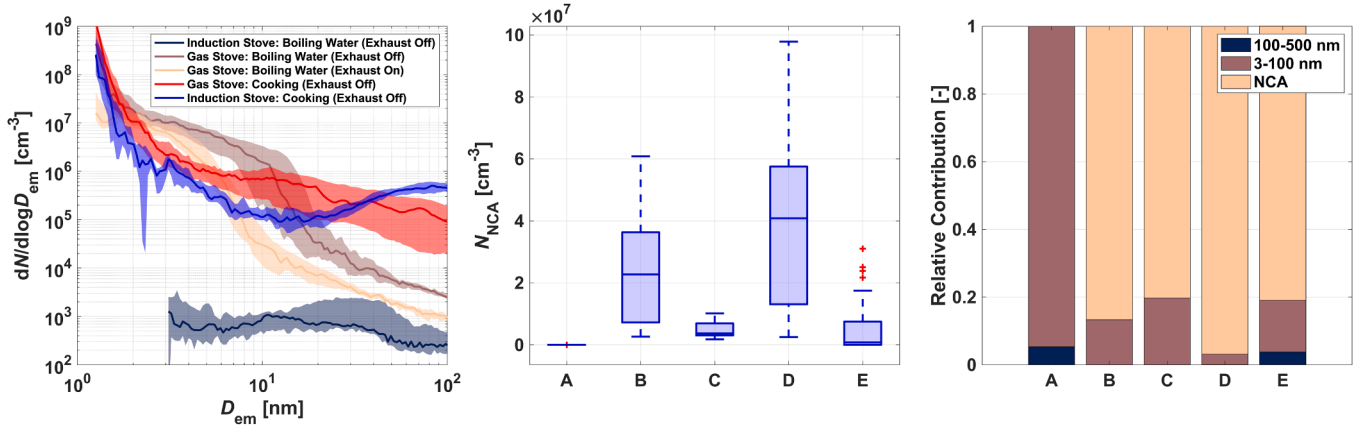

Fig. 2. Median and size-integrated indoor-originated nanoparticle emissions during isolated electric induction and gas stove use. (left column) Median indoor-originated nanoparticle number size distributions during the source emission period for isolated electric induction and gas stove use activities. The shaded area represents the 25th–75th percentile range. (middle column) Boxplots of size-integrated (1.26–3 nm) nanocluster aerosol (NCA) number concentrations during the source emission period for isolated electric induction and gas stove use activities. (right column) Median contribution of each size fraction (nanocluster aerosol (NCA; 1.26–3 nm), 3–100 nm, and 100–500 nm) to the total indoor-originated nanoparticle number concentration during the source emission period for isolated induction and gas stove use activities. The letters on the x-axis represent – A: boiling water on the electric induction stove; B: boiling water on the gas stove; C: boiling water on the gas stove with the kitchen exhaust hood operating at the medium setting (~167 ft^3 min^{-1} (283 m^3 h^{-1})); D: cooking grilled cheese sandwiches on the gas stove; and E: cooking grilled cheese sandwiches on the electric induction stove.

zEDGE test house to replicate typical daily household activities systematically, once exclusively with electric-based appliances and once with combustion-based appliances (Tables S1 and S2). Indoor-originated nanoparticle emissions were continuously monitored throughout each day with the PSMPS and SMPS, enabling a direct, real-world comparison of nanoparticle pollution across energy systems.

The first comparison focused on coffee preparation: boiling water using a gas stove vs. brewing coffee with an electric coffee pot. While the electric coffee pot showed no detectable increase in indoor-originated nanoparticle emissions (Fig. 3), boiling water on the gas stove significantly elevated nanoparticle concentrations, exceeding 10^5 nanoparticles cm^{-3}, particularly below 10 nm. Therefore, the electric coffee pot provided a significant advantage over the traditional method of boiling water on a gas stove, effectively eliminating a burst of indoor-originated nanoparticle emissions.

Next, we examined breakfast preparation, comparing pancakes cooked on a gas stove against waffles prepared using an electric waffle maker, alongside lemonade preparation. Lemonade preparation involved squeezing lemons, emitting limonene, a reactive terpene known to rapidly react with indoor atmospheric ozone and initiate new particle formation events that form nanoparticles as small as ~1 nm, growing swiftly to ~100 nm [7,35,36]. On both test days, lemonade preparation alone elevated indoor-originated nanoparticle concentrations to over 10^6 nanoparticles cm^{-3}, underscoring a critical non-combustion nanoparticle source in the kitchen. Even more importantly, residual limonene present in indoor air perpetuated continuous nanoparticle formation long after lemon squeezing had ended, sustaining elevated sub-3 nm NCA concentrations through repeated bursts of nucleation events (Fig. 3).

However, the subsequent cooking activity profoundly altered these nucleation events, demonstrating an interplay between primary (cooking) and secondary (lemonade) nanoparticle emissions. Pancakes cooked on the gas stove initially emitted sub-3 nm NCA, most likely originating from the stove's flame. However, within minutes, emissions shifted toward larger cooking-associated nanoparticles (3–100 nm), with median concentrations exceeding 10^5 nanoparticles cm^{-3} in this size range. These larger particles rapidly enhanced the surface-area-dependent scavenging effect [4,37,38], effectively depleting smaller NCA through coagulation and halting the ongoing nucleation [39] initiated during lemonade preparation.

In contrast, waffle preparation using the electric appliance produced considerably fewer large nanoparticles in the 3–100 nm size range, approximately an order of magnitude lower than the gas stove. With fewer large particles present, the scavenging of smaller sub-3 nm NCA was minimal. Consequently, continuous nucleation initiated during lemonade preparation persisted for nearly 30 additional minutes, maintaining sustained indoor-originated sub-3 nm NCA concentrations exceeding 10^6 NCA cm^{-3}. This interplay reveals the inherent complexity in evaluating nanoparticle emissions beyond simple, isolated appliance comparisons. At first glance, the electric waffle maker appears advantageous due to lower direct emissions of larger (3–100 nm) nanoparticles; however, this reduction paradoxically prolongs the persistence of smaller sub-3 nm NCA from secondary nanoparticle sources, such as limonene-driven nucleation. Conversely, the gas stove's higher emissions of larger nanoparticles substantially increase coagulation scavenging rates, effectively suppressing the persistence of secondary sub-3 nm NCA. Thus, a clear yet counterintuitive trade-off emerges: combustion cooking produces higher concentrations of larger nanoparticles, whereas electric appliances, despite lower direct emissions, may sustain elevated concentrations of smaller indoor-originated NCA. These findings underscore the importance of considering complex interactions between primary appliance emissions and secondary nanoparticle sources when assessing the exposure implications of shifting from combustion to electric appliances, especially given the ubiquity of secondary nanoparticle sources in indoor environments [40,41].

Cleaning activities with scented cleaners present notable secondary

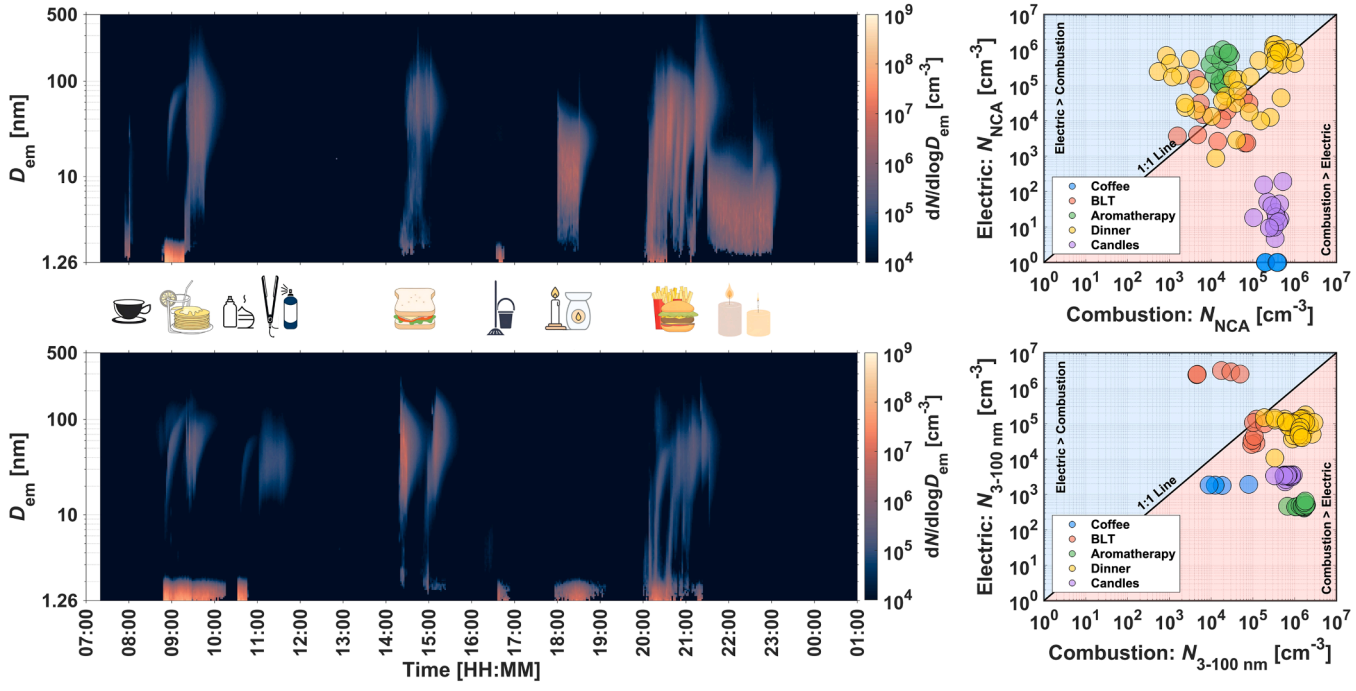

Fig. 3. Full-day time-resolved indoor-originated nanoparticle emissions and activity-based comparisons between combustion- and electric-based appliance use. The left column shows time-resolved indoor-originated nanoparticle emissions throughout the day, corresponding to common indoor activities. The top row represents the day with activities primarily involving combustion-based appliances, while the bottom row represents the day with activities using primarily electric-based appliances. Major activities are indicated with icons placed between the plots, corresponding to their respective time periods. Detailed descriptions of the activities on both days are provided in Tables S1 and S2. The right column presents a comparison of size-integrated indoor-originated nanoparticle number concentrations during specific activities from both days, plotted relative to the 1:1 line. The top row shows size integration in the nanocluster aerosol (NCA; 1.26–3 nm) size fraction, and the bottom row shows size integration in the 3–100 nm size fraction.

nanoparticle sources [7]. We observed that mopping with scented cleaners increased indoor-originated nanoparticle concentrations up to ~10^5 nanoparticles cm^{-3}, predominantly within the sub-3 nm NCA size range. Likewise, indoor fragrance products displayed distinct nanoparticle emission profiles depending on their chemical composition. A non-terpene-based air freshener showed negligible effects on indoor-originated nanoparticle concentrations, whereas using a terpene-based essential oil diffuser resulted in substantial nanoparticle generation, elevating levels to approximately 10^6 nanoparticles cm^{-3} due to terpene-ozone reactions. Personal care routines provided another illustrative example. Applying hair spray without heat produced no detectable increase in nanoparticle concentrations yet introducing heat via an electric hair straightener raised nanoparticle levels to ~10^4 nanoparticles cm^{-3} [2]. These examples underscore how common non-cooking sources, often overlooked in air quality assessments, can meaningfully contribute to elevated indoor atmospheric nanoparticle levels.

A striking contrast emerged when comparing scented candles with electric wax warmers, both used to fragrance indoor spaces but employing fundamentally different mechanisms. Combustion-driven scented candles emitted substantial indoor-originated nanoparticles primarily in the 3–100 nm size range, whereas the electric wax warmer released comparable nanoparticle concentrations (~10^5–10^6 nanoparticles cm^{-3}) dominated by much smaller nanoparticles in the sub-3 nm NCA size fraction, resulting from terpene-ozone reactions (Fig. 3). This reveals an important distinction between combustion-based candles and electric wax warmers: similar total nanoparticle concentrations, yet markedly different size distributions with distinct indoor-to-outdoor nanoparticle flux profiles.

Lunch preparation further highlighted the trade-offs between combustion and electric appliances. Both combustion and electric methods were evaluated by preparing BLT sandwiches: bread toasted on a gas stove vs. an electric toaster, and bacon cooked on a gas stove versus vs. in an electric oven. Each appliance produced distinct nanoparticle emission events, yet peak indoor-originated nanoparticle concentrations remained comparable across methods, reaching 10^5–10^6 nanoparticles cm^{-3} (Fig. 3). Interestingly, toasting bread with the electric toaster generated higher nanoparticle emissions within the 3–100 nm size range compared to gas stove toasting.

Dinner preparations reiterated these complexities. Cooking burgers and French fries on a gas stove, as well as using a combination of an induction stove, electric grill, and air fryer, resulted in nanoparticle emissions spanning both the sub-3 nm NCA and the 3–100 nm size ranges. While gas cooking emitted marginally more nanoparticles in the 3–100 nm size fraction (10^5–10^6 nanoparticles cm^{-3}) compared to electric cooking (~10^5 nanoparticles cm^{-3}), sub-3 nm NCA concentrations were similar between the two methods (10^3–10^5 NCA cm^{-3}). Thus, as observed during isolated cooking activities, electric induction cooking did not demonstrate a clear advantage over gas cooking in terms of indoor-originated nanoparticle emissions for high temperature, oil-based cooking.

However, substituting combustion-based candles with LED candles during dinner provided a definitive reduction in indoor-originated nanoparticle emissions. Traditional candles significantly increased indoor-originated nanoparticle concentrations (~10^5–10^6 nanoparticles cm^{-3}), whereas LED candles produced no measurable nanoparticle emissions, delivering the same ambiance without combustion-driven nanoparticle release (Fig. 3).

Overall, these comparisons indicate that indoor atmospheric nanoparticle emissions are strongly influenced by process-driven factors, and that replacing combustion appliances with electric alternatives may not necessarily reduce indoor-originated nanoparticle emissions under certain conditions. Fig. 3, right panel, illustrates these complexities by summarizing size-integrated indoor-originated nanoparticle concentrations relative to a 1:1 line throughout the day for combustion-based appliances and their electric alternatives. Nanoparticle emission trade-offs vary considerably across size ranges and activity types. For instance, sub-3 nm NCA emissions from both combustion and electric appliances generally approached the 1:1 line; however, electric wax warmers emitted higher NCA concentrations compared to combustion-based scented candles. Conversely, in the 3–100 nm size range, combustion appliances generally produced higher emissions; nevertheless, activities such as electric toaster use generated higher nanoparticle concentrations than gas stove toasting. Notably, nanoparticle emissions from non-cooking activities, including scented cleaning products, often matched or exceeded those from cooking. Collectively, these findings suggest that the effectiveness of electrification in reducing indoor nanoparticle pollution depends strongly on the specific activities and operating conditions involved.

3.3. *Cumulative inhalation exposure to indoor-originated nanoparticles during electric and combustion household activities*

Indoor-originated nanoparticle concentrations showed substantial increases and multiple distinct peaks across both the combustion- and electric-based activity days (Fig. 4). Although the nanoparticle emission size distributions differed depending on the activity type, peak indoor-originated nanoparticle concentrations generally occurred within similar orders of magnitude on both days (Fig. 4). Notable exceptions included coffee preparation, where boiling water on the gas stove produced a significant nanoparticle peak, whereas the electric coffee maker emitted no detectable indoor-originated nanoparticles. Similarly, combustion-based candles released substantial indoor-originated nanoparticles, whereas LED candles did not. Conversely, electric appliances such as the essential oil diffuser and electric hair straightener produced indoor-originated nanoparticle peaks absent during the use of non-terpene-based air fresheners and hair spray without heating.

The multisource nanoparticle emissions significantly influenced human inhalation exposure within the indoor environment. We quantified this exposure by calculating the cumulative respiratory tract deposited doses for occupants, utilizing measured indoor-originated nanoparticle concentrations alongside established size-resolved respiratory deposition fractions [26,42]. Deposited nanoparticle doses were assessed across three distinct regions of the adult respiratory tract: head airways, tracheobronchial region, and pulmonary region.

Cumulative nanoparticle deposition in occupants' respiratory tracts was elevated across both combustion and electric appliance use under the conditions examined. A key difference emerged during morning coffee preparation: on the combustion-based day, occupants inhaled approximately 10^{10} deposited nanoparticles, substantially above background levels (~10^8 deposited nanoparticles), while the electric coffee maker maintained inhalation doses near background conditions. However, following breakfast preparation, cumulative nanoparticle inhalation dose surged on both days, reaching the high-10^{11} deposited nanoparticles range.

Subsequent indoor activities on the electric-based day, specifically sustained nucleation from residual limonene (post-lemonade preparation), essential oil diffuser operation, and hair straightener use, further elevated total inhaled nanoparticles, surpassing 10^{12} deposited nanoparticles by midday. In contrast, the absence of similarly potent indoor atmospheric nanoparticle sources during the combustion-based day resulted in slightly lower cumulative nanoparticle inhalation. Lunch preparation and subsequent cleaning with a terpene-based cleaning product elevated nanoparticle inhalation dose further on both days. Yet, total inhaled nanoparticles through afternoon activities remained consistently higher on the electric-based day compared to the combustion-based day (Fig. 4). Across these activities, nanoparticles predominantly deposited within the head airways region (~70%), followed by the tracheobronchial region (~20%) and pulmonary region (~10%).

During evening activities, aromatherapy markedly altered regional nanoparticle deposition patterns. On the combustion-based day, burning

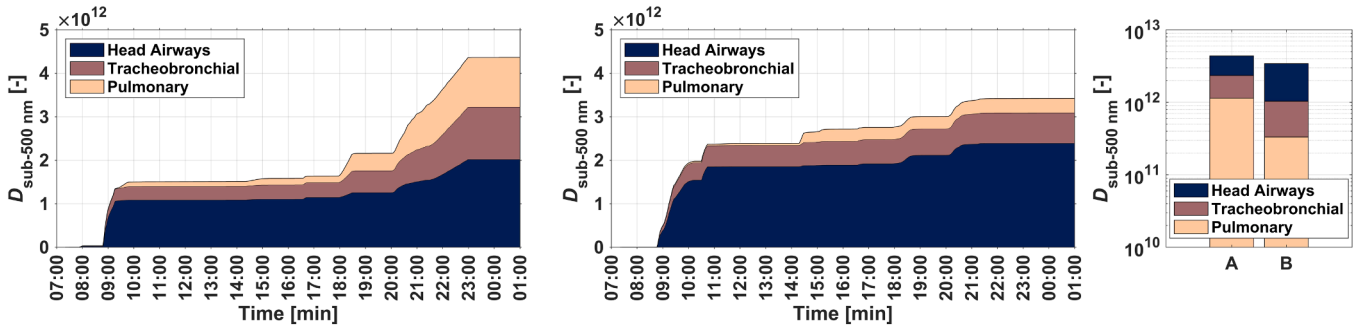

Fig. 4. Comparing indoor-originated nanoparticle exposure from combustion- vs. electric-based appliance use. The left two panels show the cumulative adult respiratory tract deposited doses over the course of the day. The two panels on the left are divided into two columns: the left column corresponds to the day with activities primarily involving combustion-based appliances, and the right column corresponds to the day with activities primarily involving electric-based appliances. The panel on the right summarizes the total respiratory tract deposited nanoparticle dose at the end of each day. The letters on the x-axis represent, A: the day with combustion-based appliance use; and B: the day with electric-based appliance use.

scented candles primarily emitted nanoparticles in the 3–100 nm size range, known for deeper respiratory penetration and greater pulmonary deposition [7,43]. Conversely, electric wax warmers predominantly generated sub-3 nm NCA, characterized by a higher deposition fraction in the head airways region [7,43]. Consequently, despite comparable total nanoparticle inhalation during aromatherapy, pulmonary nanoparticle deposition notably increased on the combustion-based day, rising from approximately 10% in the afternoon to nearly 18% post-aromatherapy, whereas pulmonary deposition remained relatively unchanged on the electric-based day.

Following dinner preparation, total inhaled nanoparticle doses remained high and comparable across both days (3.4×10^{12} deposited nanoparticles) compared to the combustion-based day (3.2×10^{12} deposited nanoparticles). However, the inhalation exposure patterns shifted again during post-dinner candlelit activities. On the combustion-based day, continued use of traditional candles further elevated inhaled nanoparticle doses. In contrast, LED candles, used on the electric-based day, emitted no detectable indoor-originated nanoparticles, resulting in negligible additional inhalation. Consequently, total cumulative nanoparticle inhalation on the combustion-based day ultimately surpassed the electric-based day, reaching 4.4×10^{12} deposited nanoparticles by the end of the combustion-based day vs. 3.4×10^{12} deposited nanoparticles by the end of the electric-based day.

Electric appliance use did not result in a clear decrease in total nanoparticle inhalation under the conditions examined, consistent with the dominant influence of process-driven emissions. However, although final cumulative inhalation doses were similarly high for both combustion- and electric-based days, distinct differences emerged in regional deposition patterns. On the electric-based day, nanoparticles primarily deposited in the head airways region (~70%), substantially exceeding that on the combustion-based day (~45%). Conversely, the combustion-based day exhibited higher pulmonary deposition (~25%) relative to the electric-based day (~10%), due to the prevalence of larger nanoparticles emitted during combustion processes.

These results suggest that, although building electrification eliminates combustion-related emissions, its effect on the overall inhaled nanoparticle dose and regional deposition patterns may depend strongly on specific activities and operating conditions. This is particularly important given the differing health implications of regional deposition: larger nanoparticles tend to deposit in the pulmonary region, while smaller nanoparticles, although largely retained in the head airways, may translocate to the brain [9,10]. Consequently, strategies focused solely on replacing combustion appliances with electric alternatives may not fully address indoor nanoparticle exposure, as emissions are strongly governed by process-driven factors rather than fuel type alone, and secondary indoor nanoparticle sources can contribute substantially under certain conditions.

3.4. Indoor-to-outdoor nanoparticle fluxes from electric and combustion household activities: urban air quality implications

Gas stoves, widely used in homes [44], emit substantial indoor atmospheric nanoparticles from both combustion and high-temperature cooking processes. As demonstrated in Section 3.1, electric induction cooktops, despite removing combustion-related emissions, generated comparably high nanoparticle concentrations during high-temperature, fat-based cooking, driven primarily by the thermal decomposition of oils rather than the energy source. Regardless of appliance type, these indoor-originated nanoparticles are ultimately transported outdoors, contributing to urban nanoparticle pollution.

Indoor-originated nanoparticles are transported outdoors via building exhaust pathways, extending their impact beyond indoor exposure and contributing to urban nanoparticle pollution. We quantified indoor-to-outdoor nanoparticle fluxes (nanoparticles min^{-1}) using directly measured nanoparticle concentrations and the test house air exchange rate (Eqs. 1–4), finding substantial fluxes for both combustion- and electric-based days (Fig. 5). During household activities, indoor-to-outdoor fluxes were on the order of 10^{12}–10^{13} nanoparticles min^{-1} for both days, comparable to reported cooking-related neighborhood emission rates (~10^{12} nanoparticles min^{-1}) [45] and exceeding reported nanoparticle exhaust fluxes from office buildings (~10^{10} nanoparticles min^{-1}) [46].

The indoor-to-outdoor flux estimation method expressed in Eqs. 1–4 provides a simple and effective approach that avoids explicitly calculating nanoparticle generation rates, as measured indoor nanoparticle concentrations inherently reflect the balance between source emissions and removal processes within the indoor environment. To validate this approach, we compared our flux estimates against an independent calculation using nanoparticle generation rates reported by Patra et al. [8], who evaluated the same electric wax warmer in the same test house under identical nominal outdoor air ventilation rates, reporting an average nanoparticle formation rate of approximately 1200 cm^{-3} s^{-1}. Using this nanoparticle formation rate, the room volume, and the mean nanoparticle transport efficiency from Figure S4, the estimated indoor-to-outdoor flux of indoor-originated nanoparticles from scented wax melt use is 4.1×10^{12} nanoparticles min^{-1}. Using Eqs. 1–4, the corresponding average indoor-to-outdoor nanoparticle flux obtained during scented wax melt use in this study is 3.6×10^{12} nanoparticles min^{-1}. This agreement supports the validity of the flux estimation approach used here.

Normalized by building footprint, indoor-to-outdoor nanoparticle fluxes on both days (~7×10^{10}–7×10^{11} nanoparticles m^{-2} min^{-1}) were at least an order of magnitude higher than reported fluxes from urban traffic (~6×10^{9} nanoparticles m^{-2} min^{-1}) [47] and exceeded biogenic new particle formation fluxes in forested environments (~3×10^{8}

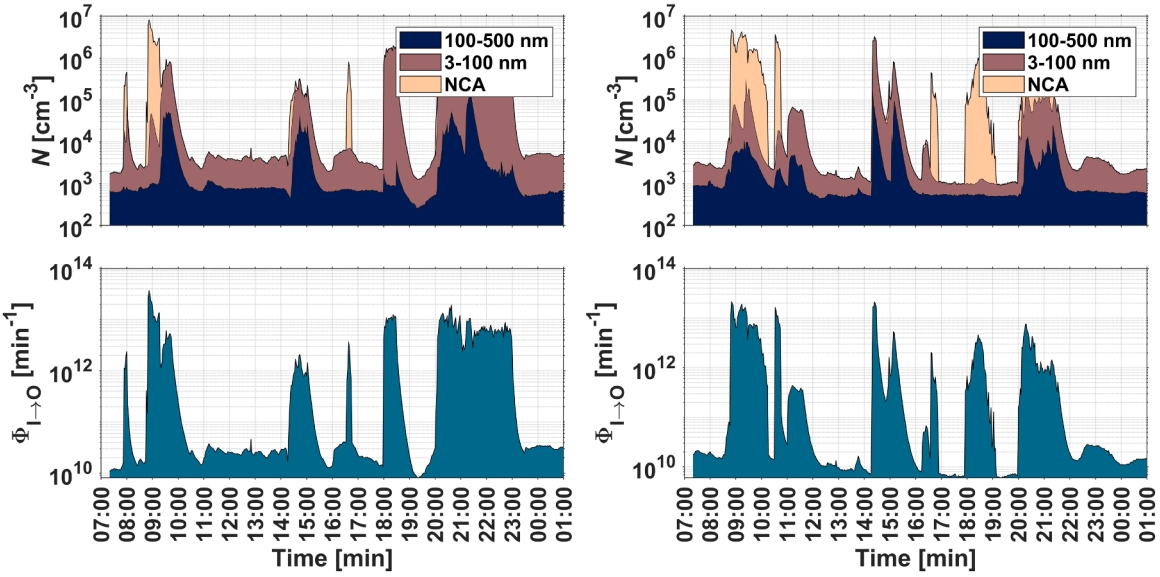

Fig. 5. Comparing indoor-to-outdoor nanoparticle fluxes from combustion- vs. electric-based appliance use. The top two panels show the size-integrated indoor-originated nanoparticle number concentrations throughout the day, color-coded according to their respective size-integration intervals: nanocluster aerosol (NCA; 1.26–3 nm), 3–100 nm, and 100–500 nm. The bottom two panels show the estimated indoor-to-outdoor nanoparticle fluxes over the course of the day. The four panels are divided into two columns: the left column corresponds to the day with activities primarily involving combustion-based appliances, and the right column corresponds to the day with activities primarily involving electric-based appliances.

nanoparticles m^{-2} min^{-1}) [48]. In dense urban settings with multistory residential buildings, overlapping emissions from vertically stacked residential units would further amplify these fluxes. These results demonstrate that residential indoor-originated nanoparticle emissions, regardless of appliance energy source, represent a significant and potentially underappreciated source of urban outdoor nanoparticle pollution, the magnitude of which depends on specific household activities and operating conditions.

4. Conclusion

Our results highlight the complexities and trade-offs involved in transitioning from combustion-based appliances to electric alternatives under the specific residential conditions examined in this study. In particular, electric induction cooktops produced indoor-originated nanoparticle concentrations comparable to gas stoves during high-temperature, oil-based cooking, demonstrating that nanoparticle formation is strongly driven by the thermal decomposition of oils rather than the energy source alone. Both appliance types generated substantial quantities of previously uncharacterized sub-3 nm NCA under these conditions, a size fraction largely absent from prior indoor nanoparticle assessments, with significant implications for inhalation exposure and respiratory tract deposition.

Our full-day assessment further revealed a complex interplay between primary appliance emissions and secondary nanoparticle formation, leading to size-dependent differences in emissions and exposure across the activities examined. The impact of electrification on indoor nanoparticle pollution was highly activity-dependent: while electrification eliminates combustion-related emissions, it does not necessarily reduce nanoparticle concentrations or inhalation exposures under the conditions examined here, particularly when high-temperature, oil-based cooking or secondary nanoparticle sources are present.

Overall, these results underscore the importance of accounting for process-driven emissions, including thermal processes and chemical transformations, when evaluating indoor nanoparticle exposures and indoor-to-outdoor nanoparticle transport in residential environments. Mitigation strategies addressing both primary and secondary nanoparticle sources, rather than focusing solely on appliance electrification, are essential for meaningfully reducing residential nanoparticle exposure and limiting contributions to urban outdoor nanoparticle pollution.

Our findings should be interpreted with several limitations in mind. PSMPS-based measurements of sub-3 nm NCA carry intrinsic uncertainties due to composition-dependent sensitivity and charger-ion interactions [4,19,49]; although our stringent 99th percentile correction improves confidence in the reported size distributions, true NCA concentrations may be underestimated. Additionally, we do not evaluate source-specific toxicological properties, and toxicological evidence for non-combustion nanoparticles remains limited. Third, the interpretation of sustained NCA formation partly relies on secondary formation pathways involving volatile organic compounds and indoor oxidants; future work including full-day measurements of indoor atmospheric volatile organic compounds and O_3 would provide additional insight into the underlying mechanisms of nanoparticle nucleation and growth. Fourth, the combustion-only and electricity-only activity patterns compared here provide a useful mechanistic contrast, but many real households, particularly in developing countries, use electric and combustion appliances concurrently or sequentially. As nanoparticle interactions appear to play an important role, future studies incorporating mixed-energy-use scenarios would enhance the real-world relevance of these findings. Finally, this study focuses on nanoparticle emissions and does not capture reductions in other combustion-related air pollutants (e.g., CO, CO_2, NO, NO_2, CH_4) achieved through electrification, which must be considered when assessing overall air quality and public health impacts.

5. Environmental Implications

This study demonstrates that indoor atmospheric nanoparticle emissions, inhalation exposures, and indoor-to-outdoor transport are substantially influenced by residential activities performed with both electric and combustion appliances. High-temperature, oil-based cooking, regardless of appliance energy source, generated indoor atmospheric nanoparticle concentrations on the order of 10^7 nanoparticles cm^{-3}, including abundant sub-3 nm nanocluster aerosol. Cumulative daily inhalation doses reached ~10^{12} deposited nanoparticles under both combustion and electric appliance scenarios, highlighting

comparable respiratory exposure risks across energy systems. Indoor-to-outdoor nanoparticle fluxes of 10^{12}–10^{13} nanoparticles min^{-1} demonstrate that residences act as persistent sources of nanoparticles to urban air, with magnitudes rivaling traffic emissions. Collectively, these findings indicate that electrification alone is unlikely to reduce indoor atmospheric nanoparticle pollution, as emissions and exposures are strongly governed by thermally and chemically driven processes rather than fuel type.

CRediT authorship contribution statement

Satya S. Patra: Writing – review & editing, Writing – original draft, Visualization, Validation, Methodology, Investigation, Funding acquisition, Formal analysis, Data curation, Conceptualization. **Chunxu Huang:** Writing – review & editing, Visualization, Methodology, Data curation. **Brian H. Magnuson:** Methodology, Data curation. **Brandon Emil Boor:** Writing – review & editing, Writing – original draft, Visualization, Validation, Supervision, Software, Resources, Project administration, Methodology, Investigation, Funding acquisition, Formal analysis, Data curation, Conceptualization. **Nusrat Jung:** Writing – review & editing, Writing – original draft, Visualization, Validation, Supervision, Software, Resources, Project administration, Methodology, Investigation, Funding acquisition, Formal analysis, Data curation, Conceptualization.

Declaration of Competing Interest

The authors declare the following financial interests/personal relationships which may be considered as potential competing interests: Brandon Emil Boor reports financial support was provided by the National Science Foundation. Nusrat Jung reports financial support was provided by Purdue University. Satya S. Patra reports financial support was provided by the American Society of Heating, Refrigerating, and Air Conditioning Engineers. Given his/her/their role as Editor of *Journal of Hazardous Materials*, Brandon Emil Boor had no involvement in the peer review of this article and had no access to information regarding its peer review. Full responsibility for the editorial process for this article was delegated to another journal editor. If there are other authors, they declare that they have no known competing financial interests or personal relationships that could have appeared to influence the work reported in this paper.

Acknowledgement

Financial support was provided by the National Science Foundation (CBET-1847493 to B.E.B.), Purdue University start-up funds (to N.J.), and an American Society of Heating, Refrigerating, and Air Conditioning Engineers Graduate Student Grant-In-Aid Award (to S.S.P.).

Appendix A. Supporting information

Supplementary data associated with this article can be found in the online version at doi:10.1016/j.jhazmat.2026.142011.

Data availability

Data will be made available on request.

References

[1] Zhu, S., Mac Kinnon, M., Carlos-Carlos, A., Davis, S.J., Samuelsen, S., 2022. Decarbonization will lead to more equitable air quality in California. Nat Commun 13, 5738. https://doi.org/10.1038/s41467-022-33295-9.

[2] Liu, J., Jiang, J., Patra, S.S., Ding, X., Huang, C., Cross, J.N., Magnuson, B.H., Jung, N., 2025. Indoor nanoparticle emissions and exposures during heat-based hair styling activities. Environ Sci Technol 59, 17103–17115. https://doi.org/10.1021/acs.est.4c14384.

[3] Marlon, J., Mildenberger, M., Burns, C., Lazarovic, S., Ballew, M., Rosenthal, S., Maibach, E., Kotcher, J., Leiserowitz, A., 2023. How many Americans want an electric home? Yale Program Clim Change Commun.

[4] Patra, S.S., Jiang, J., Ding, X., Huang, C., Reidy, E.K., Kumar, V., Price, P., Keech, C., Steiner, G., Stevens, P., Jung, N., Boor, B.E., 2024. Dynamics of nanocluster aerosol in the indoor atmosphere during gas cooking. PNAS Nexus 3, pgae044. https://doi.org/10.1093/pnasnexus/pgae044.

[5] Jathar, S.H., Sharma, N., Bilsback, K.R., Pierce, J.R., Vanhanen, J., Gordon, T.D., Volckens, J., 2020. Emissions and radiative impacts of sub-10 nm particles from biofuel and fossil fuel cookstoves. Aerosol Sci Technol 54, 1231–1243. https://doi.org/10.1080/02786826.2020.1769837.

[6] Li, J., Zhao, H., Russell, M.L., Delp, W.W., Johnson, A., Tang, X., Walker, I.S., Singer, B.C., 2024. Air pollutant exposure concentrations from cooking a meal with a gas or induction cooktop and the effectiveness of two recirculating range hoods with filters. Indoor Environ 1, 100047. https://doi.org/10.1016/j.indenv.2024.100047.

[7] Patra, S.S., Liu, J., Jiang, J., Ding, X., Huang, C., Keech, C., Steiner, G., Stevens, P. S., Jung, N., Boor, B.E., 2024. Rapid nucleation and growth of indoor atmospheric nanocluster aerosol during the use of scented volatile chemical products in residential buildings. ACS EST Air 1, 1276–1293. https://doi.org/10.1021/acsestair.4c00118.

[8] Patra, S.S., Jiang, J., Liu, J., Steiner, G., Jung, N., Boor, B.E., 2025. Flame-free candles are not pollution-free: scented wax melts as a significant source of atmospheric nanoparticles. Environ Sci Technol Lett 12, 175–182. https://doi.org/10.1021/acs.estlett.4c00986.

[9] Kreyling, W.G., Hirn, S., Möller, W., Schleh, C., Wenk, A., Celik, G., Lipka, J., Schäffler, M., Haberl, N., Johnston, B.D., Sperling, R., Schmid, G., Simon, U., Parak, W.J., Semmler-Behnke, M., 2014. Air–blood barrier translocation of tracheally instilled gold nanoparticles inversely depends on particle size. ACS Nano 8, 222–233. https://doi.org/10.1021/nn403256v.

[10] Oberdörster, G., Sharp, Z., Atudorei, V., Elder, A., Gelein, R., Kreyling, W., Cox, C., 2004. Translocation of inhaled ultrafine particles to the brain. Inhal Toxicol 16, 437–445. https://doi.org/10.1080/08958370490439597.

[11] Jiang, J., Ding, X., Tasoglou, A., Huber, H., Shah, A.D., Jung, N., Boor, B.E., 2021. Real-time measurements of botanical disinfectant emissions, transformations, and multiphase inhalation exposures in buildings. Environ Sci Technol Lett 8, 558–566. https://doi.org/10.1021/acs.estlett.1c00390.

[12] Jiang, J., Ding, X., Isaacson, K.P., Tasoglou, A., Huber, H., Shah, A.D., Jung, N., Boor, B.E., 2021. Ethanol-based disinfectant sprays drive rapid changes in the chemical composition of indoor air in residential buildings. J Hazard Mater Lett 2, 100042. https://doi.org/10.1016/j.hazl.2021.100042.

[13] Jiang, J., Ding, X., Patra, S.S., Cross, J.N., Huang, C., Kumar, V., Price, P., Reidy, E. K., Tasoglou, A., Huber, H., Stevens, P.S., Boor, B.E., Jung, N., 2023. Siloxane emissions and exposures during the use of hair care products in buildings. Environ Sci Technol 57, 19999–20009. https://doi.org/10.1021/acs.est.3c05156.

[14] Liu, J., Jiang, J., Ding, X., Patra, S.S., Cross, J.N., Huang, C., Kumar, V., Price, P., Reidy, E.K., Tasoglou, A., Huber, H., Stevens, P.S., Boor, B.E., Jung, N., 2024. Real-time evaluation of terpene emissions and exposures during the use of scented wax products in residential buildings with PTR-TOF-MS. Build Environ 255, 111314. https://doi.org/10.1016/j.buildenv.2024.111314.

[15] G. Steiner H. Flentje M. Väkevä L. Keck J. Vanhanen Monitoring ambient aerosol size distributions from 1 to 55 nm with the GRIMM-AIRMODUS PSMPS. EGU General Assembly Conference Abstracts EGU 2021 EGU21 12472.

[16] Jiang, J., Jung, N., Boor, B.E., 2021. Using building energy and smart thermostat data to evaluate indoor ultrafine particle source and loss processes in a net-zero energy house. ACS EST Eng 1, 780–793. https://doi.org/10.1021/acsestengg.1c00002.

[17] Patra, S.S., Ramsisaria, R., Du, R., Wu, T., Boor, B.E., 2021. A machine learning field calibration method for improving the performance of low-cost particle sensors. Build Environ 190, 107457. https://doi.org/10.1016/j.buildenv.2020.107457.

[18] Kangasluoma, J., Cai, R., Jiang, J., Deng, C., Stolzenburg, D., Ahonen, L.R., Chan, T., Fu, Y., Kim, C., Laurila, T.M., Zhou, Y., Dada, L., Sulo, J., Flagan, R.C., Kulmala, M., Petäjä, T., Lehtipalo, K., 2020. Overview of measurements and current instrumentation for 1–10 nm aerosol particle number size distributions. J Aerosol Sci 148, 105584. https://doi.org/10.1016/j.jaerosci.2020.105584.

[19] Kangasluoma, J., Junninen, H., Lehtipalo, K., Mikkilä, J., Vanhanen, J., Attoui, M., Sipilä, M., Worsnop, D., Kulmala, M., Petäjä, T., 2013. Remarks on ion generation for CPC detection efficiency studies in sub-3-nm size range. Aerosol Sci Technol 47, 556–563. https://doi.org/10.1080/02786826.2013.773393.

[20] Patra, S.S., Steiner, G., Boor, B.E., 2026. Fate of 1–6 nm candle combustion nanoparticles in indoor atmospheric environments. Environ Sci Technol 60, 834–846. https://doi.org/10.1021/acs.est.5c05577.

[21] Wu, T., Tasoglou, A., Wagner, D.N., Jiang, J., Huber, H.J., Stevens, P.S., Jung, N., Boor, B.E., 2024. Modern buildings act as a dynamic source and sink for urban air pollutants. Cell Rep Sustain 1, 100103. https://doi.org/10.1016/j.crsus.2024.100103.

[22] J.E. Brockmann Aerosol Transport in Sampling Lines and Inlets, Aerosol Measurement: Principles, Techniques, and Applications, 3rd Edition 2011 68 105.

[23] P. Kulkarni P.A. Baron K. Willeke Fundamentals of Single Particle Transport, Aerosol Measurement: Principles, Techniques, and Applications, 3rd Edition; 15-30 2011.

[24] Hussein, T., Boor, B.E., Löndahl, J., 2020. Regional inhaled deposited dose of indoor combustion-generated aerosols in Jordanian urban homes. Atmosphere 11. https://doi.org/10.3390/atmos11111150.

[25] Wu, T., Täubel, M., Holopainen, R., Viitanen, A.-K., Vainiotalo, S., Tuomi, T., Keskinen, J., Hyvärinen, A., Hämeri, K., Saari, S.E., Boor, B.E., 2018. Infant and adult inhalation exposure to resuspended biological particulate matter. Environ Sci Technol 52, 237–247. https://doi.org/10.1021/acs.est.7b04183.
[26] Miller, F.J., Asgharian, B., Schroeter, J.D., Price, O., 2016. Improvements and additions to the multiple path particle dosimetry model. J Aerosol Sci 99, 14–26. https://doi.org/10.1016/j.jaerosci.2016.01.018.
[27] Sankhyan, S., Zabinski, K., O'Brien, R.E., Coyan, S., Patel, S., Vance, M.E., 2022. Aerosol emissions and their volatility from heating different cooking oils at multiple temperatures. Environ Sci Atmos 2, 1364–1375. https://doi.org/10.1039/D2EA00099G.
[28] Zhang, D.-C., Liu, J.-J., Jia, L.-Z., Wang, P., Han, X., 2019. Speciation of VOCs in the cooking fumes from five edible oils and their corresponding health risk assessments. Atmos Environ 211, 6–17. https://doi.org/10.1016/j.atmosenv.2019.04.043.
[29] Katragadda, H.R., Fullana, A., Sidhu, S., Carbonell-Barrachina, Á.A., 2010. Emissions of volatile aldehydes from heated cooking oils. Food Chem 120, 59–65. https://doi.org/10.1016/j.foodchem.2009.09.070.
[30] Zhang, Z., Zhu, W., Hu, M., Wang, H., Chen, Z., Shen, R., Yu, Y., Tan, R., Guo, S., 2021. Secondary organic aerosol from typical chinese domestic cooking emissions. Environ Sci Technol Lett 8, 24–31. https://doi.org/10.1021/acs.estlett.0c00754.
[31] Masoud, C.G., Li, Y., Wang, D.S., Katz, E.F., DeCarlo, P.F., Farmer, D.K., Vance, M. E., Shiraiwa, M., Hildebrandt Ruiz, L., 2022. Molecular composition and gas-particle partitioning of indoor cooking aerosol: insights from a FIGAERO-CIMS and kinetic aerosol modeling. Aerosol Sci Technol 56, 1156–1173. https://doi.org/10.1080/02786826.2022.2133593.
[32] Cummings, B.E., Pothier, M.A., Katz, E.F., DeCarlo, P.F., Farmer, D.K., Waring, M. S., 2023. Model framework for predicting semivolatile organic material emissions indoors from organic aerosol measurements: applications to HOMEChem stir-frying. Environ Sci Technol 57, 17374–17383. https://doi.org/10.1021/acs.est.3c04183.
[33] Wang, Q., Wang, S., Gao, X., Wang, X., Liao, H., Zhao, L., Zhong, F., Yang, Y., 2025. Breathing better: how range hood operation rates affect vertical centralized exhaust in Chinese residential kitchens. J Build Eng 108, 112953. https://doi.org/10.1016/j.jobe.2025.112953.
[34] Rim, D., Wallace, L., Nabinger, S., Persily, A., 2012. Reduction of exposure to ultrafine particles by kitchen exhaust hoods: the effects of exhaust flow rates, particle size, and burner position. Sci Total Environ 432, 350–356. https://doi.org/10.1016/j.scitotenv.2012.06.015.
[35] Pagonis, D., Algrim, L.B., Price, D.J., Day, D.A., Handschy, A.V., Stark, H., Miller, S. L., de Gouw, J.A., Jimenez, J.L., Ziemann, P.J., 2019. Autoxidation of limonene emitted in a University Art Museum. Environ Sci Technol Lett 6, 520–524. https://doi.org/10.1021/acs.estlett.9b00425.
[36] Vartiainen, E., Kulmala, M., Ruuskanen, T.M., Taipale, R., Rinne, J., Vehkamäki, H., 2006. Formation and growth of indoor air aerosol particles as a result of d-limonene oxidation. Atmos Environ 40, 7882–7892. https://doi.org/10.1016/j.atmosenv.2006.07.022.
[37] Cai, R., Häkkinen, E., Yan, C., Jiang, J., Kulmala, M., Kangasluoma, J., 2022. The effectiveness of the coagulation sink of 3–10nm atmospheric particles. Atmos Chem Phys 22, 11529–11541. https://doi.org/10.5194/acp-22-11529-2022.
[38] Cai, R., Yang, D., Fu, Y., Wang, X., Li, X., Ma, Y., Hao, J., Zheng, J., Jiang, J., 2017. Aerosol surface area concentration: a governing factor in new particle formation in Beijing. Atmos Chem Phys 17, 12327–12340. https://doi.org/10.5194/acp-17-12327-2017.
[39] Gong, Y., Hu, M., Cheng, Y., Su, H., Yue, D., Liu, F., Wiedensohler, A., Wang, Z., Kalesse, H., Liu, S., Wu, Z., Xiao, K., Mi, P., Zhang, Y., 2010. Competition of coagulation sink and source rate: new particle formation in the Pearl River Delta of China. Atmos Environ 44, 3278–3285. https://doi.org/10.1016/j.atmosenv.2010.05.049.
[40] Steinemann, A., 2015. Volatile emissions from common consumer products. Air Qual Atmos Health 8, 273–281. https://doi.org/10.1007/s11869-015-0327-6.
[41] Nematollahi, N., Kolev, S.D., Steinemann, A., 2019. Volatile chemical emissions from 134 common consumer products. Air Qual Atmos Health 12, 1259–1265. https://doi.org/10.1007/s11869-019-00754-0.
[42] Manojkumar, N., Srimuruganandam, B., Shiva Nagendra, S.M., 2019. Application of multiple-path particle dosimetry model for quantifying age specified deposition of particulate matter in human airway. Ecotoxicol Environ Saf 168, 241–248. https://doi.org/10.1016/j.ecoenv.2018.10.091.
[43] Rosales, C.M.F., Jiang, J., Lahib, A., Bottorff, B.P., Reidy, E.K., Kumar, V., Tasoglou, A., Huber, H., Dusanter, S., Tomas, A., Boor, B.E., Stevens, P.S., 2022. Chemistry and human exposure implications of secondary organic aerosol production from indoor terpene ozonolysis. Sci Adv 8, eabj9156. https://doi.org/10.1126/sciadv.abj9156.
[44] Kashtan, Y., Nicholson, M., Finnegan, C.J., Ouyang, Z., Garg, A., Lebel, E.D., Rowland, S.T., Michanowicz, D.R., Herrera, J., Nadeau, K.C., Jackson, R.B., 2025. Nitrogen dioxide exposure, health outcomes, and associated demographic disparities due to gas and propane combustion by U.S. stoves. Sci Adv 10, eadm8680. https://doi.org/10.1126/sciadv.adm8680.
[45] Zhao, Y., Liu, L., Tao, P., Zhang, B., Huan, C., Zhang, X., Wang, M., 2019. Review of effluents and health effects of cooking and the performance of kitchen ventilation. Aerosol Air Qual Res 19, 1937–1959. https://doi.org/10.4209/aaqr.2019.04.0198.
[46] Wagner, D.N., Jung, N., Boor, B.E., 2025. Spatiotemporal mapping of ultrafine particle fluxes in an office HVAC system with a diffusion charger sensor array. ACS EST Air 2, 49–63. https://doi.org/10.1021/acsestair.4c00140.
[47] Straaten, A., Meier, F., Scherer, D., Weber, S., 2022. Significant reduction of ultrafine particle emission fluxes to the urban atmosphere during the COVID-19 lockdown. Sci Total Environ 838, 156516. https://doi.org/10.1016/j.scitotenv.2022.156516.
[48] Pryor, S.C., Barthelmie, R.J., Larsen, S.E., Sørensen, L.L., 2017. Ultrafine particle number fluxes over and in a deciduous forest. J Geophys Res Atmospheres 122, 405–422. https://doi.org/10.1002/2016JD025854.
[49] Kangasluoma, J., Kontkanen, J., 2017. On the sources of uncertainty in the sub-3nm particle concentration measurement. J Aerosol Sci 112, 34–51. https://doi.org/10.1016/j.jaerosci.2017.07.002.